The Sevilla Powder Tester: A Tool for Characterizing the Physical Properties of Fine Cohesive Powders at Very Small Consolidations[†]

A. Castellanos, J.M. Valverde, and M.A.S. Quintanilla
*Facultad de Física. Universidad de Sevilla**

Abstract

We present a fluidized bed apparatus that enables us to test the bulk mechanical properties such as the yield stresses and compressibility of fine cohesive powders. Every measurement is preceded by driving the powder into the bubbling regime in which the material loses memory of its previous history. Then the gas flow is set to a given value to take the powder into a well defined and reproducible initial state of low consolidation. Reverse flow is used to exert high compressive stress. A cornerstone of our technique is that the procedure is automatized, thus making results operator insensitive. Besides being a practical tool to diagnose the flowability of experimental powders, the Sevilla Powder Tester (SPT) also provides us with a powerful technique to research fundamental problems in powder mechanics.

1 Introduction

The mass flow of fine particles is relevant in many industrial fields. It is estimated that 60% of products in the chemical industry are manufactured as particulates and a further 20% use powders as ingredients [1]. In spite of this, most industrial powder processes are dependent on empirical correlations since the link between the physics of local grain interactions and their global mechanical behavior is still poorly understood. A clear example are fluidized beds, which are extensively used whenever a good solid-fluid contact is needed such as in the catalytic cracking of oil, the combustion of coal, drying, mixing, transport, etc. A precise knowledge of the fluidized bed structure and behavior is quite relevant not only from a theoretical point of view but also from the practical point of view.

The behavior of powders can be significantly influenced by particle size, particle deformation, distribution of forces, cohesive and frictional interaction, contact restructuring, aggregation, interstitial gas, etc. The presence of these multiple and usually cooperative features makes the problem of investigating powder behavior from a fundamental perspective a rather complicated challenge, thus empirical approaches prevail. Most of the empirical studies to characterize powder flow yield numbers which are not clearly related to the fundamental physical properties. More importantly, due to the hysteretic nature of interparticle contact forces, uniform powders are hard to create and the packing arrangement is a strong function of the previous history. Generally speaking, the techniques employed lack a satisfactory way of initializing the powder in order to have an initial reproducible state in which the memory of the powder has been erased. Moreover, the more cohesive the powder, the larger the memory effects are. Consequently, the wide experimental variations in bulk properties at low consolidations measured by the traditional testers preclude a reliable estimation of interparticle forces [2], which are ultimately responsible for the ability of a powder to flow [3].

In this paper we review a Powder Tester apparatus [4] in which the powder sample is conveniently initialized by the use of fluidization. This Powder Tester enables us to investigate fluidization properties such as bed expansion, sedimentation, aggregation of fine particles within the fluidized bed, onset of bubbling for sufficiently large gas flow, transition to a solid-like regime for gas flows smaller than a critical one, etc [5]. For the solid state, in which particle contacts are permanent, the tester measures the uniaxial tensile yield stress of the powder and its average particle volume fraction as a function of the consolidation stress,

* Avenida Reina Mercedes s/n, 41012 Sevilla. Spain.
† Accepted: August 26, 2004

which can be controlled in a range spanning from a few to thousands of Pascal by means of forward and reverse controlled gas flow. The behavior of powders during compaction yields information about the mechanism of density increase. From the bulk stresses, we estimate the interparticle contact forces that are well correlated to direct measurements of forces between isolated particles made using a Scanning Force Microscope (SFM) [6]. All the measurements can be done under complete computer control and are fully automated. A further advantage of the SPT for testing experimental powders is that the instrument only needs a small volume of powder (typically around 20 g.).

1.1 Some techniques of analysing powder flowability

Schwedes recently made an extensive review on testers for measuring the bulk flow properties of granular materials [7]. In this section, we highlight some of the most-used techniques in powders from a critical perspective.

1.1.1 Empirical techniques

A traditional way of testing powder flowability is to measure the ability of the powder to flow through standard devices. For example, we find in the *Book of the American Society for Testing and Materials Standards* a technique that consists of measuring the time that a given mass of powder takes to discharge through a hopper [8]. Even though this technique has been proved to be useful for metallic powders, an external energy source such as tapping is needed for very cohesive powders to help powder flow [9]. Vibration, however, may consolidate the powder and, especially in the case of fine particles, this enhances cohesiveness. A similar technique, frequently used for pharmaceutical tabletting applications, consists of forcing the powder to pass through rings of decreasing diameters [10]. The flowability index is defined as the diameter of the smaller ring through which the sample can discharge three consecutive times. There is also a commercial rheometer similar to the ones employed to measure the viscosity of liquids, but that has been adapted to test powder flow [11]. The rheometer incorporates a blade with different sections in the opposite sides of a rotation shaft. The first section has its surface parallel to the rotation shaft whereas the second section is twisted relative to the rotation shaft. The Hosokawa Powder Tester [12] is another instrument that has been extensively employed in the xerographic industry to measure toner flowability. In the Hosokawa test, a number of screens of different sizes are placed vertically and are vibrated. An estimation of the toner flowability is given by the relative mass of powder that passes through each screen.

The success of these techniques is hindered by the difficulty of initializing the powder in an initial reproducible state. Therefore, results are dependent on the history of the powder: i.e. the filling procedure, previously applied stresses, etc. This is particularly important in the case of fine cohesive powders for which interparticle attractive forces may increase by several orders of magnitude with the applied external load [13]. An additional problem is that the interaction of the powder with mechanical parts, such as the blade of a rheometer, may produce a "heterogenous" cohesiveness since the load and shear applied can change abruptly from point to point within the sample. Thus the results achieved depend on the particular design of the device and on the experimental procedure. In addition, the correlation of the experimental results to fundamental physical parameters of the powder remains rather obscure. Therefore, it would be desirable to measure properties more directly linked to fundamental parameters, thus yielding more robust and confident results.

1.1.2 Techniques of analysing powder flowability based on fundamental properties

The powder compressibility has usually been taken as a measure of powder flowability [14]. Granular materials that flow well end up in very dense packings that are quite difficult to compress, whereas poorly flowing powders pack in open structures that can be further compressed with ease. Compaction tests in which a cylindrical plug of powder is compacted axially by a piston are commonly used in civil engineering [15]. A proposed number to classify powder flowability is the Hausner ratio, defined as the ratio of the tapped powder density to the untapped powder density [16].

Most of the situations involving the flow of powders imply the presence of shear stresses. Therefore, some techniques to test powder flowability are focused on measuring the yield stress as the powder sample is sheared. Consider an arbitrary plane through the powder sample and a shear stress τ acting on that plane; there will be a value of stress that will cause the powder to shear off in the plane and cause the powder to flow. This yield stress depends on the normal stress σ acting perpendicular to the plane. In general, τ increases with σ, and the relationship between

τ and σ defines the yield locus of the powder. At high stresses the yield locus can be approximated by a linear function known as Coulomb's law [17]

$$\tau = \sigma \tan \Phi + c \quad (1)$$

where c and Φ are the cohesion and the angle of internal friction. For many coarse granular materials c is negligible.

The point of the yield locus on the negative σ axis is the ultimate tensile strength σ_t. The linear theory is, however, inadequate to describe the behavior of fine cohesive powders at low values of σ and τ that occur in practice. Traditionally, the Jenike shear cell [18] has been used by engineers in powder technology to estimate the angle of internal friction of highly consolidated granular materials. Essentially, the technique consists of compacting a powder sample with a known external load into a cylindrical cell composed of two metal rings one upon the other. With the compaction load still applied, the minimum steady state shear stress necessary to displace the upper ring horizontally with respect to the lower one is measured. Steady state flow means flow at constant density and constant shear stress. These values of normal and shear stresses define the end point of the yield locus. Then the normal load on the powder is decreased and the new horizontal force necessary to initiate shearing of the powder is measured. In order to minimize the influence of the operator, the Jenike cell is commercialized with a reference material with which researchers can check both their equipment and experimental technique. The reference powder consists of "3 kg of limestone powder packed in a polyethylene jar" and is accompanied by a certificate that supplies the limiting shear stress for four different powder normal stresses [19]. However, in a great deal of powder processing equipment there is no significant compressive force while the Jenike cell is inappropriate for low consolidation stresses. The recently developed ring shear tester represents a technical improvement on the Jenike tester in order to measure the yield locus at smaller loads ($<\sim$100 Pa) [20]. An experimental problem that besets the Jenike cell technique and its modified versions is the lack of a reliable method of producing reproducible initial states. Interparticle contact forces are very sensitive to small variations of the previous external loads. As a result, errors due to poor preparation methods can easily arise. Further disadvantages of the Jenike test are that it must be accepted that the slip plane coincides with a horizontal plane and that the shear process takes place uniformly throughout the sample in order to relate the stresses to the real stresses inside the material. This is known to be false for overconsolidated materials [21]. A commercial alternative to the Jenike shear cell is the Peschl annular shear cell, in which the shear stress is applied by rotating the top part of an annular shear box containing the powder sample [21]. While this test allows for a constant area of shear and unlimited shear distance, making it useful for quantifying powder flow after failure, wall effects and strong uncertainty in stress distribution are major drawbacks.

Another property that has been employed to quantify powder flow is the angle of repose of a pile of powder [22]. Even though the angle of repose is a well defined property of noncohesive granular materials, it is meaningless when cohesive interaction becomes important. We may remember from our childhood that sand castles can sustain 90° slopes but when we tried to increase the size of the castle, landslides would probably happen that decreased the angle of repose to well below 90°. The influence of the size of the powder sample on the avalanching behavior of fine powders is well documented in the literature [23]. Therefore, the size of the pile, which is indeed an external parameter, must be specified in the testing procedure when dealing with cohesive powders.

A common tool to analyse the avalanching behavior of powders is a horizontal rotating drum partially filled with the granular sample [24]. In this device, intermittent and nearly reproducible avalanches are observed at low rotation speeds. For low-cohesive well-behaved granular materials, avalanches occur quite regularly with nearly uniform size and time spacing, whereas in the case of poorly flowing cohesive powders, the time spacing and size of avalanches shows a noisy behavior [24]. A rotating drum-based unit, developed by Kaye and coworkers [25], is now commercially available. In this device, avalanches are automatically detected by a change in the light intensity captured by a grid of photocells placed behind the drum. The avalanching behavior is characterized by the time interval between consecutive avalanches. The scatter of the points is a measure of the regularity of the avalanche process. With this technique, a gas conditioning system can be implemented [26] in order to control gas conditions inside the chamber that may have a profound effect on powder flowability. Testing cohesive powders is, however, difficult and the test usually yields inaccurate results. A source of error is that the powder sticks easily to the walls of the drum and this reduces visibility. As a result, the light intensity series can easily become

non-stationary whereas the number of avalanches per unit time detected decreases, thus complicating analysis of the data. In the case of very cohesive powders it is also likely that the powder slips as a whole. A further criticism is that merely the data on the time interval between consecutive avalanches cannot be enough to analyse cohesive systems with complex dynamics. For instance, Quintanilla et al. [24] have seen that for a class of cohesive powders, there is a regular sequence of large avalanches preceded by a number of two or three small precursors. In such cases, an in-depth statistical analysis is needed.

Since flowability is closely linked to interparticle forces, it can be thought that a good bulk test is to measure the powder tensile yield stress for which the interparticle attractive force is responsible. The split cell tester is a commercial device able to measure a tensile yield stress [21]. The sample is held in a ring-shaped cell and is compacted vertically using a plunger. Then a horizontal tensile stress is applied and steadily increased until the sample is pulled apart. In this way, the tensile yield stress for a given consolidation stress is measured. In the lifting lid tester, the sample is pulled vertically in the same direction of compaction [21]. These techniques present some inconveniences when applied to fine cohesive powders. One of them is again the lack of a mechanism for initializing the powder into a reproducible state of consolidation. As a consequence, results are of poor reproducibility. Another is the difficulty of measuring the tensile yield stress of fine cohesive powders at low consolidation stresses by means of piston consolidation [27]. It must be remarked that the way of preparation and compaction of the powder in the cell does not produce an isotropic state of stresses. Therefore, the tensile yield stress does not have to coincide with the tensile strength. Research tools such as triaxial tests achieve an approximated isotropic behavior by using hydrostatic compaction, but is applicable only to high compression loads.

1.1.3 Direct measurement of interparticle forces

A good estimation of the powder flowability should be based on direct measurement of the interparticle forces. The adhesion force between individual particles can be measured directly using a Scanning Force Microscope [6]. With this instrument, a probe particle is attached at the end of a V-shaped tipless cantilever. The probe particle is brought close to an isolated substrate particle under computer control and a loading-unloading cycle is applied. The largest downward deflection achieved by the cantilever during unloading gives the adhesion force. **Figure 1** shows the statistical distribution of the adhesion force measured between two micrometer-sized toner particles. Another apparatus recently reported to measure interparticle forces [28] comprises a sensor unit composed of a contact needle that comes into contact with the powder and dislodges particles, measuring the adhesive force between the particle and sample substrate. This technique, however, does not have a way to control the previous load force on the particle that modifies adhesion substantially for plastic contacts [6]. The same criticism applies to the well-established centrifugal method [28].

As can be seen in **Fig. 1**, the SFM data obtained for the adhesive force between irregularly shaped particles such as xerographic toners has a broad dispersion. This is mainly due to the dependence of the adhesive force on the local surface properties of the contact. When two irregular particles are brought into contact, we can expect a wide range for the adhesive force measured depending on the exact location of the contact that determines the asperity size. This problem gets worse when flow conditioner additives are dispersed on the particle surface.

1.1.4 The fluidized bed method

A method to obtain the uniaxial tensile yield stress of the powder with high reproducibility consists of supplying a gas flow into a powder bed [27, 29]. The layout of the experimental system is shown schemati-

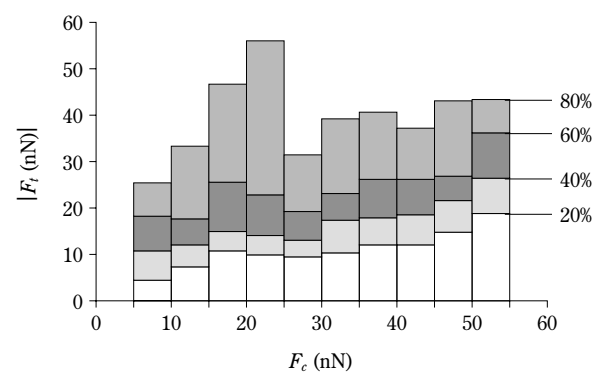

Fig. 1 Statistical distribution of the adhesive force (Ft) between two irregularly shaped toner particles with low surface additive coverage as a function of the load force (Fc). Forces are measured using a Scanning Force Microscope. The vertical bars indicate the cumulative distributions of the experimental measurements for every range of load force.

cally in **Figure 2**. Powder samples are supported on a porous plate in a vertically-oriented cylindrical vessel. Our experimental materials are xerographic toners made of polymer and with typical particle size ~10 μm. Pore size of the distributor plate is ~5 μm to ensure that toner particles do not penetrate into the pores and that the gas stream is distributed uniformly over the lower boundary of the bed. A controlled flow of dry nitrogen is introduced into the lower part of the vessel. By using dry nitrogen, the complicating effect of humidity, which is known to affect particle adhesion [30], is minimized. The gas flow is controlled by a mass flow controller while the gas pressure drop across the bed Δp is measured by a differential pressure transducer. Readings of the pressure drop across the porous plate (without toner in the cell) are taken before each series of powder measurements. In all the range of gas flows we used, there is a linear dependence of the pressure drop across the plate on the gas flow velocity. The powder sample is weighed and then placed in the vessel; at this stage the sample is quite inhomogeneous, with some loose and some compacted areas. To homogenize the sample, the bed is driven into the freely bubbling regime by imposing a large gas flow. Once in the bubbling regime, the bed loses memory of its previous history [31]. In the case of highly cohesive powders, such as toners with very low additive concentration, it is necessary to shake the sample in order to break up channels that conduct fluidizing gas away from the bulk of the powder and prevent fluidization. For that purpose, an electromagnetic shaker can be incorporated into the set-up in the base of the bed [4]. The bed is allowed to bubble during a time period large enough to reach a stationary state and after that the gas flow is suddenly returned to zero. This gives a repeatable starting condition for the powder. The height of the bed h provides an average value of the particle volume fraction

$$\langle \phi \rangle = \frac{m_s}{\rho_p A h} \tag{2}$$

where m_s is the powder mass, ρ_p is the particle density that must be known beforehand, and A is the cross-sectional area of the vessel. h is measured by means of an ultrasonic sensor placed on top of the vessel. The consolidation stress σ_c at the bottom of the bed is assumed to be the total weight of the sample divided by the area of the gas distributor. To measure the uniaxial tensile yield stress σ_t we subject the vertical layer of powder to an upward-directed flow of gas that is slowly increased to put the bed under tension. The total pressure drop is measured and the pressure drop across the gas distributor is subtracted from it. This is shown in **Figure 3**. When the gas passes through the packed bed of particles, the gas pressure drop is due to frictional resistance and increases linearly with increasing gas flow at low Reynolds numbers as described in general by the Carman-Kozeny equation [32]

$$\frac{dp}{dx} = \frac{E\mu}{d_p^2} \frac{\phi^2}{(1-\phi)^3} v_g, \tag{3}$$

where x is the vertical coordinate measured downward from the free surface of the bed, μ is the dynamic gas viscosity ($\mu = 1.89 \times 10^{-5}$ Pa·s at ambient temperature for dry nitrogen), v_g the superficial gas velocity, and $E \simeq 180$ is an empirical constant. There is a critical

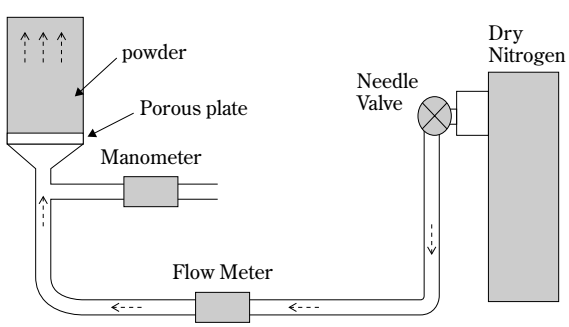

Fig. 2 Original apparatus used by us for measuring the uniaxial tensile yield stress of the powder.

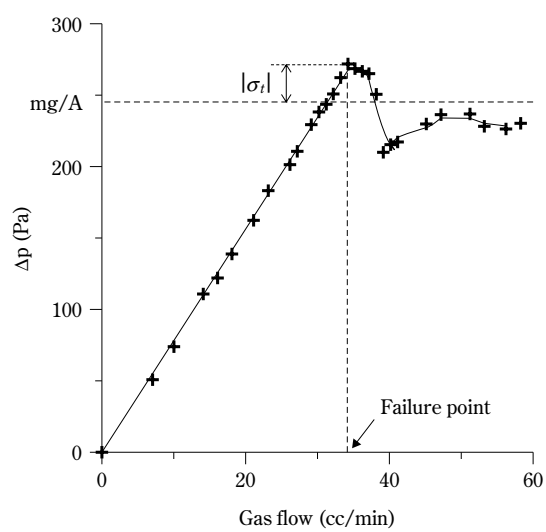

Fig. 3 Pressure drop across a bed of toner (Canon CLC500 cyan) consolidated by a consolidation stress $\sigma_c \simeq 70$ Pa. Cross-sectional area of the bed 20.3 cm^2.

gas velocity at which the powder fractures and the gas pressure drop across the bed Δp falls abruptly. In order to find the tensile yield stress it is important to know how the powder fails. Close observations reveal that fracture of the bed always starts at the lowest point, the bottom of the bed. This was already predicted theoretically and later observed by Tsinontides and Jackson [33]. In their one-dimensional analysis, they neglected the wall effect and considered the uniaxial stress σ, local particle volume fraction ϕ and gas pressure depending only on the vertical coordinate x. Next, we give a slightly modified analysis from that of Tsinontides and Jackson [33] to show explicitly that the condition for tensile yield will be first met at the lowest point of the bed as the gas flow is progressively increased.

1.1.5 Location of fracture in the fluidized bed

In the consolidated equilibrium state, prior to the application of a gas flow, there are no external forces acting upon the particles except for the gravity force. Then we have a compressive stress $\sigma_c(x)$ across the bed that obeys the simple equation

$$\frac{d\sigma_c}{dx}=\rho_p\phi g \tag{4}$$

The vertical coordinate x is measured downward from the free surface of the bed. When the gas is forced to pass through the bed, we must also consider the drag force per unit total volume F_s exerted by the gas on the particles, which is given by the gas pressure drop per unit length $F_s=dp/dx$. Then the force balance equation is

$$\frac{d\sigma}{dx}=\rho_p\phi g-\frac{dp}{dx} \tag{5}$$

Since in fine powders, the gas flow is usually at small Reynolds numbers, it is admitted that F_s is proportional to the gas velocity $F_s\approx\beta(\phi)v_g$. For a sufficiently large gas velocity, the negative contribution of the drag force will turn the stress σ negative and equal to the tensile yield stress σ_t at some point within the bed. In order to find the yield condition, Eq. 5 must be integrated. There are several empirical equations in the literature for $\beta(\phi)$. Tsinontides and Jackson found it reasonable to adopt the Richardson-Zaki equation [34]:

$$\beta(\phi)=\frac{\rho_p\phi g}{v_{p0}}\frac{1}{(1-\phi)^{n-1}} \tag{6}$$

where n is ~ 5 for small Reynolds numbers and v_{p0} is the sedimentation velocity of a single particle, $v_{p0}=(1/18)(\rho_p-\rho_g)d_p^2g/\mu$ (ρ_g is the gas density), in the Stokes regime. While Eq. 6 describes well the behavior of fluidized beds at small values of the particle volume fraction, the Carman-Kozeny equation (Eq. 3) gives the best results for $\phi>0.3$ [35]. Since we are looking for the yield point of the granular solids at large values of ϕ, Eq. 3 seems more appropriate to us for the pressure gradient. The integration of Eq. 5 yields

$$\sigma(x)=\int_0^x\rho_p\phi(\xi)g\left\{1-\frac{10\phi(\xi)}{[1-\phi(\xi)]^3}\frac{v_g}{v_{p0}}\right\}d\xi \tag{7}$$

where we have used $E=180$ and the gas density has been neglected as compared to particle density.

Let us consider first the simplest case of a homogeneous bed in which $\phi=\phi_0$ and $\sigma_t=\sigma_{t0}<0$ are constants throughout the bed. Then we have

$$\sigma(x)=\rho_p\phi_0 gx\left(1-\frac{10\phi_0}{(1-\phi_0)^3}\frac{v_g}{v_{p0}}\right) \tag{8}$$

i.e. the uniaxial stress across the bed will increase linearly with a slope that decreases as the gas velocity is increased. Eventually the slope becomes negative and with a sufficiently large gas velocity, σ will equal σ_{t0} at the point where $|\sigma|$ is maximum, which is always the bottom of the bed. Note that if σ_t increases with the depth of the bed (due to an increase in consolidation, for example) the fracture will occur also at the base of the sample as long as there is a non-vanishing σ_{t0}, at the free surface (tensile yield stress at zero consolidation).

A more realistic approach is to take into account that $\phi(\xi)$ increases with the depth of the bed as a result of the increase of the local consolidation stress. In the whole range of consolidations tested, we obtain a good fit to the experimental data on the average particle volume fraction $\langle\phi\rangle$ by the modified hyperbolic law (see as an example **Figure 4**)

$$\langle\phi\rangle(\xi)=a-\frac{b}{(1+c\xi)^d} \tag{9}$$

For the commercial toner Canon CLC700, we have $a=1.366$, $b=1.088$, $c=3.968$, and $d=0.02454$ with a regression coefficient $R=0.9954$. To apply this formula, we need to assume that the average particle volume fraction $\langle\phi\rangle(\xi)$ from the free surface to a depth ξ in a bed of total height x is equal to the measured $\langle\phi\rangle$ in a bed of total height ξ. From the definition of $\langle\phi\rangle$

$$\langle\phi\rangle(\xi)=\frac{1}{\xi}\int_0^\xi\phi(\lambda)d\lambda \tag{10}$$

we derive the local particle volume fraction $\phi(\xi)$

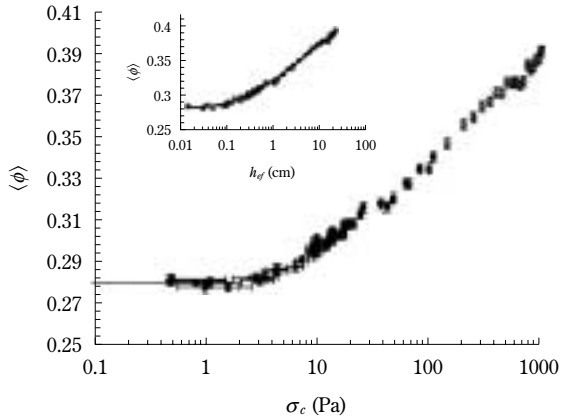

Fig. 4 Average particle volume fraction of a consolidated bed of Canon CLC700 toner as a function of the consolidation stress. The data obtained by reducing consolidation by means of an upward-directed gas flow (see below, solid symbols) are plotted jointly with data obtained by increasing consolidation by means of a downward-directed gas flow (see below, open symbols). The inset shows the whole set of data of the average particle volume fraction as a function of the effective depth measured from the top free surface, defined as $h_{ef}=\sigma_c/(\rho_p\langle\phi\rangle g)$ (the continuous curve represents the modified hyperbola fit equation $\langle\phi\rangle=a-\frac{b}{(1+ch_{ef})^d}$, with a=1.366, b=1.088, c=3.968, d=0.02454, and a regression coefficient R=0.9954).

$$\phi(\xi)=\langle\phi\rangle(\xi)+\xi\frac{d\langle\phi\rangle(\xi)}{d\xi} \tag{11}$$

to be used in Eq. 7. **Figure 5** shows the new profiles of the uniaxial stress obtained by numerical integration of Eq. 7 for different values of the gas velocity. The essential difference with respect to the uniform case is the convex shape of $\sigma(x)$ due to the increase of the drag force with depth. The consequence is that the yield condition is more neatly met at the base of the sample.

According to Eq. 5, the total gas pressure drop across a bed of height h at yield, $(\Delta p)_Y$, is given by the powder weight per unit area plus the tensile yield stress at the bottom

$$(\Delta p)_Y=\rho_p\langle\phi\rangle gh+|\sigma_t(h)| \tag{12}$$

Thus the overshoot of Δp beyond the bed weight per unit area when the powder fails gives us a quantitative measure of the uniaxial tensile yield stress $\sigma_t(h)$. For practical purposes, we checked that the tensile yield stress is not sensitive to the rate of increase of the gas flow. **Figure 6** shows results of σ_t for a given sample obtained using different rates. It is seen that the deviation between the results is within the experimental scatter (±1 Pa).

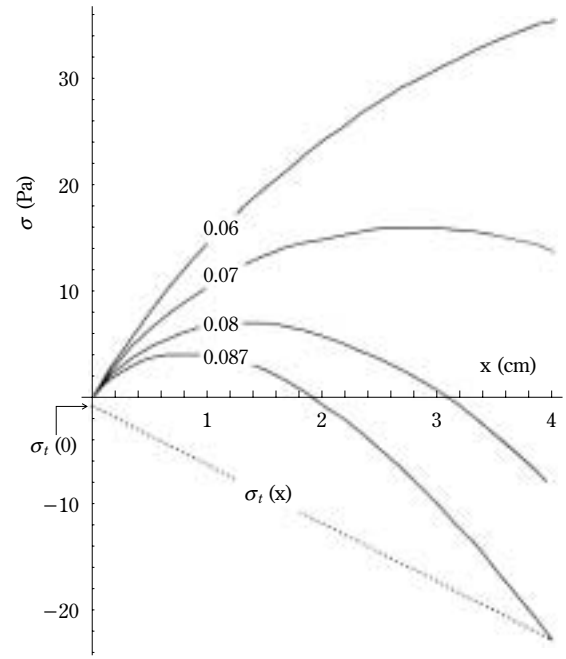

Fig. 5 Continuous lines: Uniaxial tension (σ) across a non-homogeneous bed of powder as the gas flow is increased (the ratio of the gas velocity to the sedimentation velocity of an individual particle v_g/v_{p0} is indicated for each curve). The free surface is at x=0 and the bottom at x=4 cm. The calculation is performed for a non-homogeneous bed with average particle volume fraction $\langle\phi\rangle=1.366-1.088/(1+3.968\xi)^{0.02454}$ (fit curve to Canon CLC500 toner experimental data) and particle density ρ_p=1199 kg/m^3. The dotted line is the experimental tensile yield stress (σ_t=1+5.5x Pa) for Canon CLC500. The yield condition ($\sigma=\sigma_t$) is met at the bottom of the powder (x=4 cm) for $v_g/v_{p0}\simeq 0.087$.

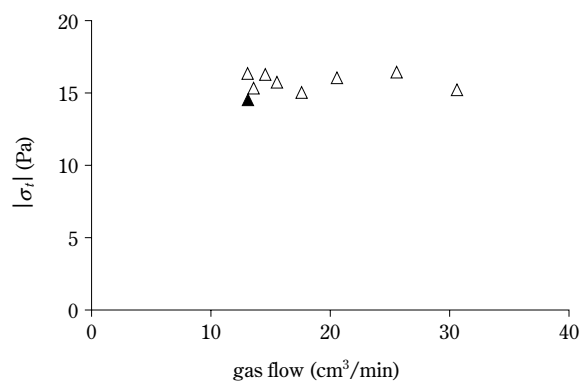

Fig. 6 Uniaxial tensile yield stress measured by increasing quasi-statically the gas flow (solid triangle) and by imposing instantaneous values (void triangles) of the gas flow represented in the horizontal axis.

As noted by Tsinontides and Jackson [33], the condition for tensile yield can be met either at the lowest point within the powder bed or at the contact between the bed and the gas distributor plate. However, we have consistently observed that the gas distributor surface remains always covered by a thin layer of powder after the break. Thus the measurement is indeed that of the tensile yield stress of the powder rather than a measure of the interface strength between the distributor plate and the powder. As further proof, we present in **Figure 7** experimental measurements of σ_t using both metallic and ceramic gas distributor plates. Within the experimental scatter, the results fit to a single curve.

The yield condition will be more neatly met at the base of the powder for the most cohesive toners ($|\sigma_t|$ large) while a large portion of powder remains far from the yield condition. In contrast, for low-cohesive systems ($|\sigma_t|$ small), the uniaxial stress will be close to the tensile yield stress throughout all the material at the yield point, therefore, in practice, the fracture will be less clearly visible at the base. In our experimental work, we observe a variety of behaviors at the yield point depending on the magnitude of the tensile yield stress and in agreement with this theoretical prediction. For most cohesive powders, the fracture at the bottom is clean and the powder rises in the bed as a plug. Furthermore, the bottom of the plug does not erode as it rises in the bed. The toner without flow additives behaves in this way. For powders of medium-large cohesiveness, fracture of the bed is still clearly visible and plugs are still formed, but the plug erodes as powder agglomerates fall away from its lower surface. The plug then becomes unstable and collapses at a certain height. Examples of this behavior are the toners with 0.01% and 0.05% Aerosil concentration by weight (12.5 μm particle size). For powders of low cohesiveness, plugs are rarely visible. After the break at the bottom of the bed, the fracture propagates until it reaches a certain height. Then, the gas escapes from the powder through channels which erupt like miniature volcanoes. The lower the cohesiveness of the toner, the less stable are the channels. These effects are observed, for example, in the toners with 0.1% and 0.2% Aerosil concentration. Finally, for the least cohesive powders, for example, the experimental toner with 0.4% Aerosil concentration or the Canon CLC500 toner, plugs do not develop, channels are very unstable, and a state of homogeneous fluidization is easily reached. We note, however, that this type of behavior depends also on the consolidation stress σ_c that influences the tensile yield stress – as we will see. In that sense, beds of small σ_c favor the formation of channels, whereas highly consolidated beds favor the formation of stable plugs.

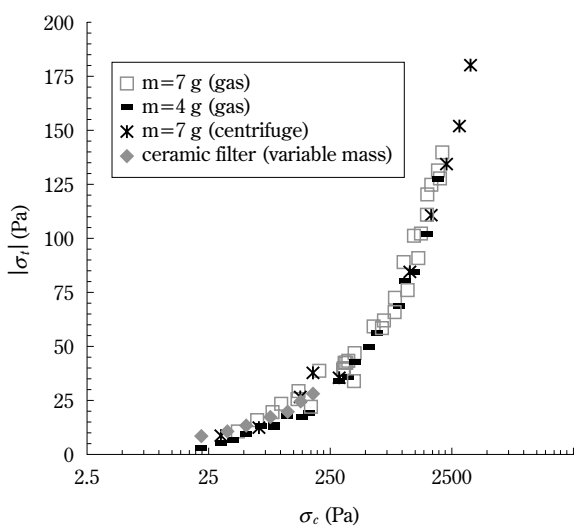

Fig. 7 Uniaxial tensile yield stress as a function of the consolidation stress for an experimental xerographic toner with 0.2% concentration by weight of additive. The data from different tests using consolidation by gas (two tests with samples of different masses) and centrifuging in a bed with a metallic gas distributor are plotted jointly with data obtained in a bed with a ceramic gas distributor where consolidation was increased by adding new mass to the sample.

Valverde et al. [27] found that wall effects are negligible for particles with a typical size of ~10 μm in beds with typical heights not larger than their diameter, as can be seen in **Figure 8**. Data of the average particle volume fraction from circular beds and from a rectangular bed fit within the experimental scatter to a single curve.

In our early investigations, two techniques were employed in order to test the powder under different consolidation stress. In the first one, the powder mass was varied by adding powder to the bed [27] (see, for example, **Fig. 8**). In the second one, the vessel with the powder inside was centrifuged prior to measuring the tensile yield stress [36], thus increasing the apparent gravity by $g_a=(g^2+\omega^4 r^2)^{0.5}$, where ω is the angular velocity and r the average radius at which the bed is rotating (see, for example, **Fig. 7**). These techniques needed to be performed by human operators and therefore none of them allowed for automation of the measurements. Furthermore, there are some difficulties related to testing the powder under very

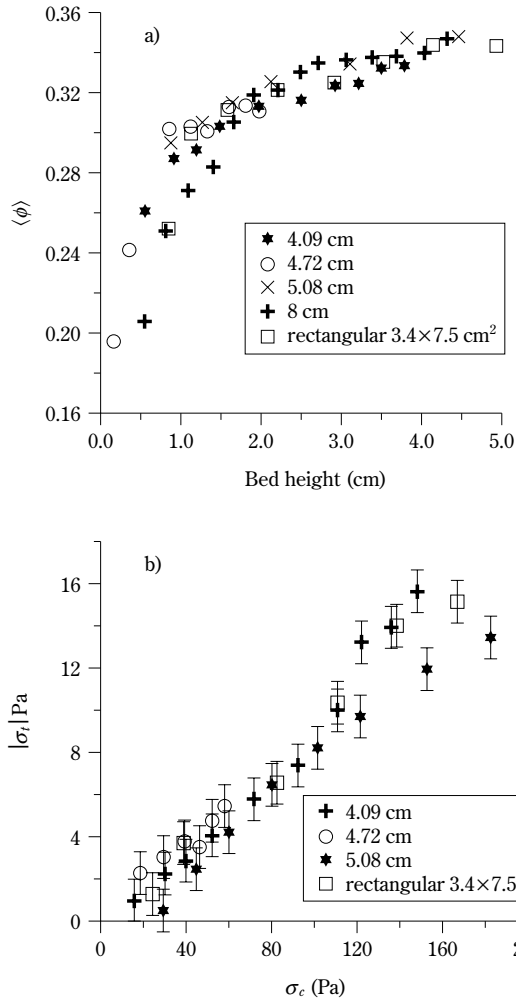

Fig. 8 (a) Average particle volume fraction as a function of the bed height. (b) Test of the uniaxial tensile yield stress versus consolidation stress. Data obtained for toner with 0.4% of additive obtained with different bed diameters (4.09 cm, 4.72 cm, 5.08 cm, 8.0 cm) and with a rectangular bed.

low/high consolidations. For very small consolidation stresses, beds of extremely low height must be used. In such cases, it was likely that non-uniform consolidation allowed the gas to flow preferentially through regions of high porosity such as channels. In the other extreme, if we wanted to achieve high consolidations by adding mass to the bed, its height should be increased up to values larger than the bed diameter for which wall effects are not negligible. In those cases, the tensile yield stress measured had an important contribution from the wall friction as shown by **Figure 9**. We will see that these inconveniences are solved by using the gas flow as an agent to compress or decompress the powder.

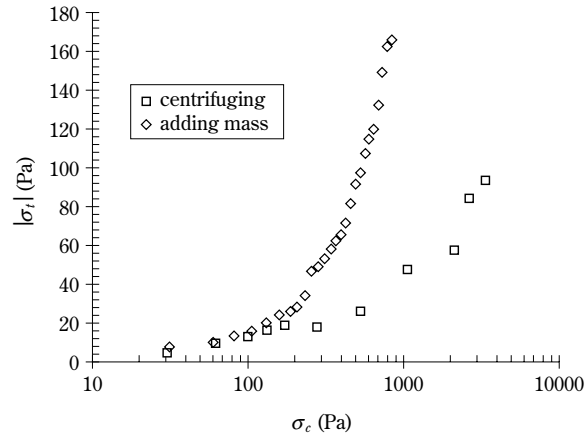

Fig. 9 Uniaxial tensile yield stress as a function of the apparent consolidation stress for the xerographic toner Canon CLC700 using different techniques of consolidation. One of them consists of adding mass to the sample contained in a cylindrical bed (diameter D=5.08 cm), where σ_c at the bottom would be given by $\rho_b\langle\phi\rangle gh$ if wall effects are neglected. The other way of consolidation consists of centrifuging the bed. With the technique of adding mass, wall effects are not negligible for σ_c>~200 Pa, corresponding to bed heights typically larger than the bed diameter ($h=\sigma_c/(\rho_b\langle\phi\rangle g)$ ~5 cm).

2 The automated Sevilla Powder Tester (SPT)

In **Figure 10** a schematic view of the automated SPT is shown. The main novelty is that by means of a series of computer-controlled valves, a controlled dry nitrogen flow can be pumped upward or downward through the bed while the gas pressure drop across the bed is read from the differential pressure transducer. In this way, the gas flow can be used to automatically vary the consolidation stress on the powder while at the same time avoiding wall effects and inhomogeneous gas distribution through shallow layers.

To compress the powder over the sample weight per unit area after the powder has settled, the valves are operated to change the gas flow path to the reverse mode. Then the downward-directed gas flow is slowly increased from zero to a given value. The gas imposes a distributed pressure over the granular assembly pressing it against the distributor plate. The consolidation stress at the base of the bed is thus increased up to

$$\sigma_c = W + \Delta p_0 \tag{13}$$

where $W=\rho_b\langle\phi\rangle gh$ and Δp_0 is the downward-directed gas pressure drop. Further increasing the compressing gas flow imposes further pressure on the sample.

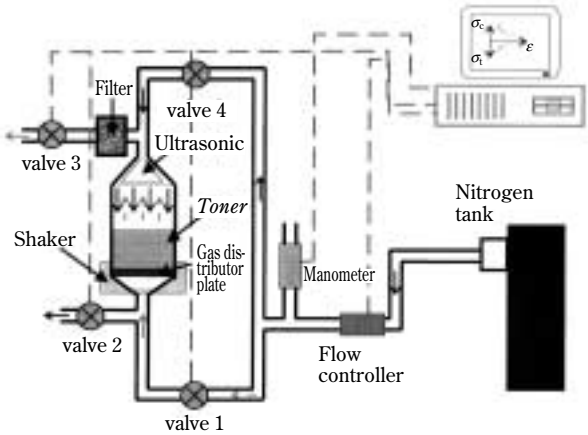

Fig. 10 Schematic diagram of the automated Powder Tester. The powder sample is held in a 4.45-cm diameter, 17-cm high cylinder made of polycarbonate, the base of which is a sintered metal gas distributor of 5 μm pore size. The cylinder is placed on a shaker used to help powder fluidization. Dry nitrogen is supplied from a tank of compressed gas and a mass flow controller is used to adjust the flow. The pressure drop across the bed is measured by a differential pressure transducer. A series of computer-controlled valves are used to control the gas flow path through the bed. The bed height is read from an ultrasonic sensor. All these components are connected to a computer by means of a data acquisition board. A filter is placed upstream of valve 3 to catch elutriated particles and prevent valve 3 from damage.

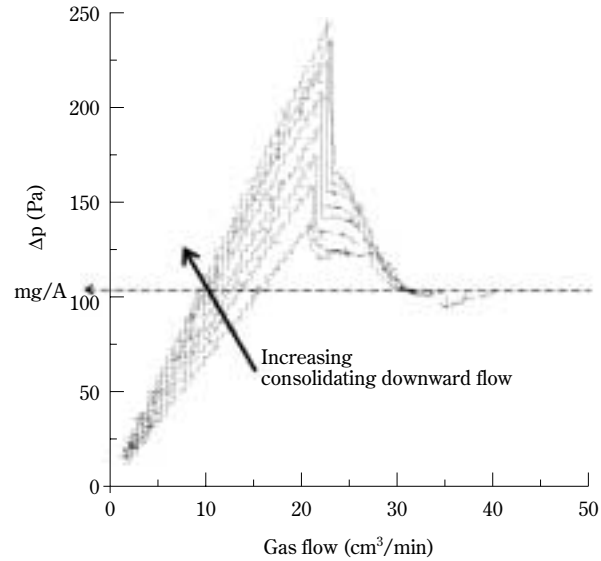

Fig. 11 Gas pressure drop versus gas flow for a given mass of xerographic toner (with 0.05%wt of silica) previously consolidated with a downward-directed gas flow. Curves in the left-hand direction correspond to increasing values of the compressing gas flow and hence to increasing values of the consolidation stress σ_c.

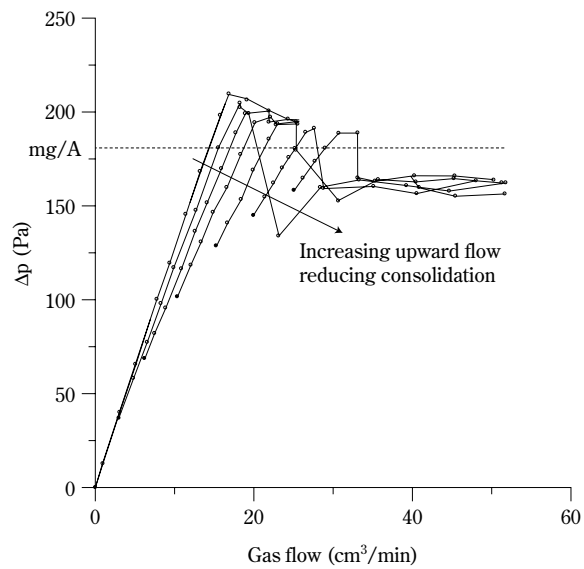

Fig. 12 Gas pressure drop versus gas flow for a given mass of xerographic toner (with 0.2%wt of silica) in states of reduced consolidation obtained by allowing the powder to settle under an upward-directed gas flow. Curves in the right-hand direction correspond to increasing values of the decompressing gas flow and hence to decreasing values of the consolidation stress σ_c.

On the other hand, the automatic Powder Tester provides us with a useful technique to test the powder under very low confining pressures like in microgravity. To decrease σ_c below the powder weight per unit area, we allow the powder to settle under a remaining upward-directed flow. In this way, σ_c is lowered down to

$$\sigma_c = W - \Delta p_0 \tag{14}$$

where Δp_0 is the pressure drop of the remaining gas flow reducing consolidation.

As before, the uniaxial tensile yield stress of the consolidated sample is measured by slowly increasing an upward-directed gas flow that subjects the bed to a tensile stress. The bed height is automatically measured by means of an acoustic pulse technique. **Figures 11** and **12** show the gas pressure drop across the bed during the breaking process for overconsolidated and underconsolidated states, respectively. As consolidation is increased, it is clearly seen that the slope of the linear part increases as a consequence of the increase of the average particle volume fraction. The overshoot of the pressure over the weight per unit area (i.e. the uniaxial tensile yield stress) also increases. Conversely, when the sample consolidation

is subsequently decreased, the average particle volume fraction decreases and hence the slope of the linear part decreases and the uniaxial tensile yield stress decreases.

Figure 13a is an example of the complete diagram than can be obtained from the SPT. It shows the interdependence between the consolidation stress, the tensile yield stress and the particle volume fraction for two powders with different levels of surface additive coverage, SAC, concentration. Clearly, a higher consolidation implies larger particle volume fraction and tensile yield stress. In the upper part of the figure it is seen that for a given consolidation stress, the particle volume fraction has a larger value for a higher additive level. This is a direct result of the increase in flowability with increasing additive, which increases the ability of the toner particles to rearrange themselves at a given stress. For a constant value of the consolidation stress, the tensile yield stress increases with decreasing additive concentration (**Figure 13b**). This is directly related to the increase in interparticle force with decreasing additive concentration [6].

The SPT has been fully automated and yields highly repeatable results [4]. This was also shown previously in **Fig. 7**, where the experimental curves $\sigma_t - \sigma_c$, obtained by means of gas consolidation and centrifugation, overlap. The data plotted in **Figure 14** also show that we cannot differentiate the results for the average particle volume fraction as a function of the consolidation stress obtained from both compaction techniques.

Figures 15 and **16** give an idea of the sensitivity of the SPT to differentiate the flowability of apparently similar powders. In **Fig. 15**, we present the phase diagrams yielded by the aeroflow meter for two samples of different color of the toner Canon CLC700 (magenta and cyan). It is difficult to establish a quantitative difference in the flowability of both samples. **Fig. 16** shows the average particle volume fraction of both samples as a function of the consolidation stress applied by the downward gas flow (Eq. 13). Now both toners are well separated. As a consequence of their better ability to flow, the magenta toner particles are able to pack in a more compact structure for the same consolidation stress and this is clearly captured by the SPT. A straightforward extension of the SPT consisting of using nitrogen with controlled relative humidity enables the characterization of powder flow under well-controlled ambient conditions.

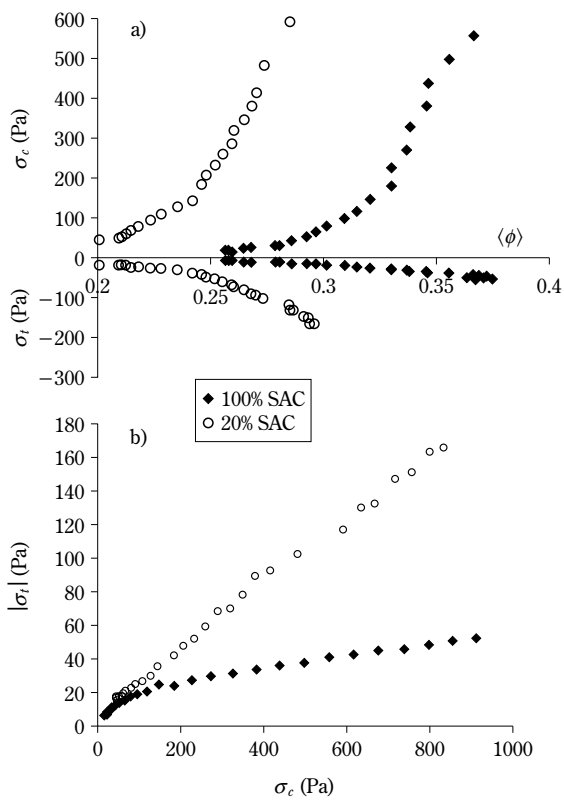

Fig. 13 (a) Relationship between the average particle volume fraction $\langle\phi\rangle$, uniaxial tensile yield stress σ_t and consolidation stress σ_c as measured by the SPT. (b) Tensile yield stress as a function of the consolidation stress. Results for two xerographic toners of ≃7 μm particle size and with different surface additive coverage (SAC) levels are shown.

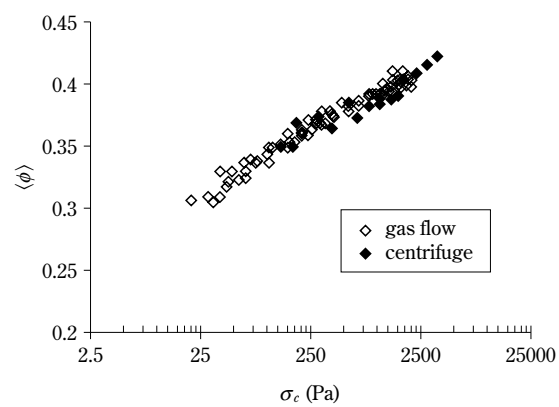

Fig. 14 Average particle volume fraction as a function of the consolidation stress for a toner of 12.5 μm particle size and 40% SAC. The external pressure is applied by means of a gas flow (void symbols) and by means of centrifugation of the cell (solid symbols).

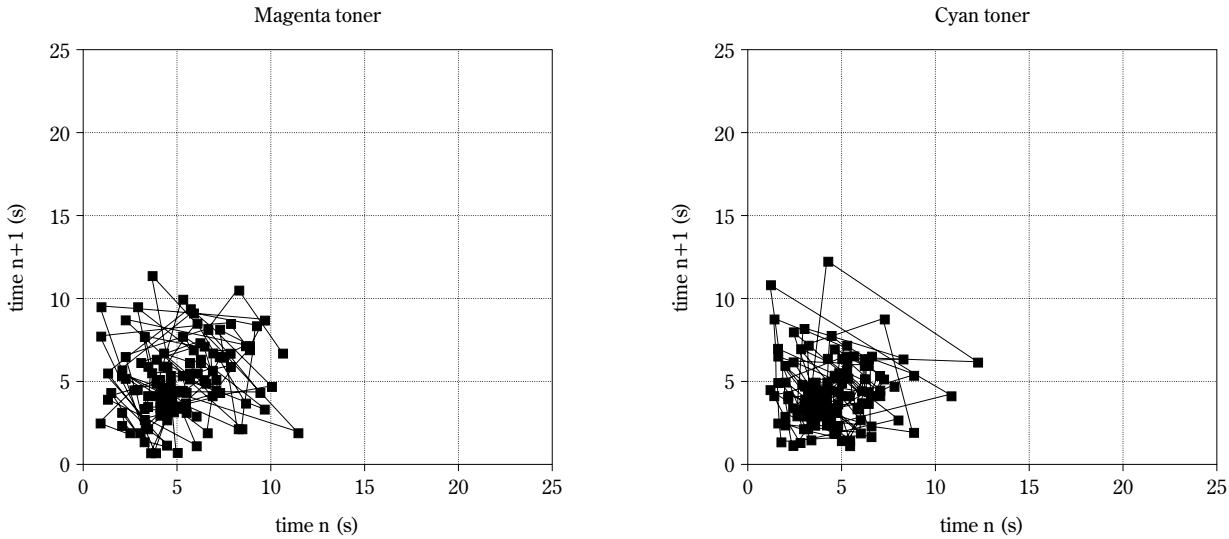

Fig. 15 Delay map for two samples of different color (magenta and cyan) of the commercial xerographic toner Canon CLC700. The points of time T_n at which an avalanche occurs are represented against the points of time T_{n+1} of the next avalanche.

2.0.6 Viscoplastic flow of interparticle contacts

An interesting experiment that can be performed automatically with the Powder Tester is to subject the sample to a fixed value of the consolidation stress for a controlled period of time. After this time period, the consolidation stress is removed and the tensile yield stress is measured. The increase of the tensile yield stress gives us an insight into the viscoplastic behavior of the interparticle contacts. From a practical point of view, the increase of strength with time of consolidation during storage is a relevant issue. Our measurements for xerographic toners indicate that the estimated adhesion force [6] rises exponentially to a maximum in a time scale that depends on the load imposed and on the surface additive coverage. **Figure 17** indicates that as the load is increased while keeping the surface additive coverage constant, the relative increase of the adhesion force becomes more

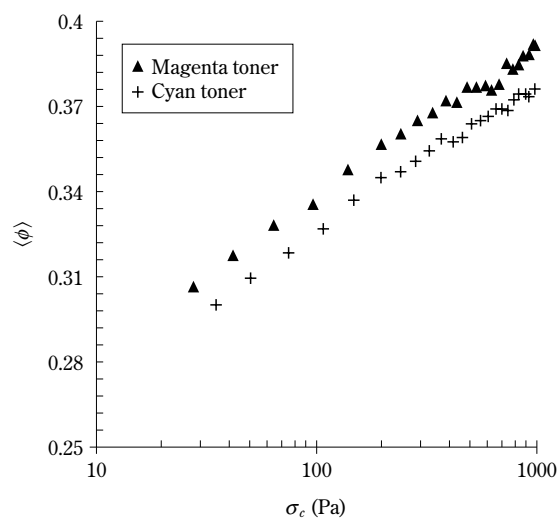

Fig. 16 Average particle volume fraction as a function of the consolidation stress measured using the SPT for two samples of different color (magenta and cyan) of the commercial xerographic toner Canon CLC700.

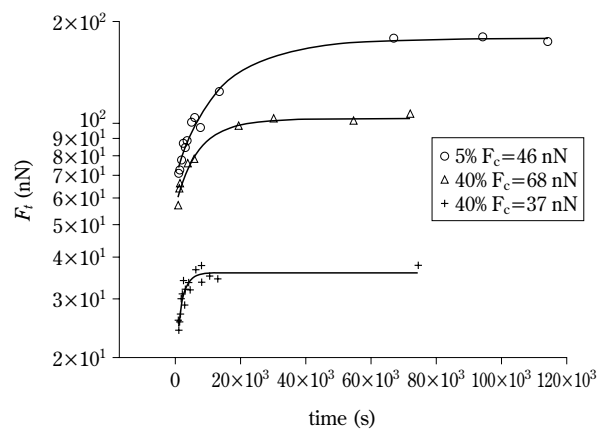

Fig. 17 Estimated interparticle adhesion force as a function of the time during which the powder is consolidated. Examples are shown for toner particles with different surface Aerosil coverage and subjected to different load forces.

pronounced. A similar behavior is obtained if the surface additive coverage is decreased while keeping the load constant. Therefore, not just the actual value of the adhesive force for a given load force but also the time of application of the force plays a role in the compression process, suggesting a viscoplastic deformation of the contact in large time scales. To avoid viscoplastic flow, the data presented in the previous sections of this paper were taken from measurements made within a short time scale (t<~5 min.).

3 The tilted fluidized bed: a technique for measuring the incipient flow of a sheared cohesive powder

Our fluidized bed technique provides a convenient method of generating a reproducibly consolidated powder and can be adapted to measure the limiting shear stress of the powder subjected to a controlled and small consolidation stress. After initializing, the next step is to apply a shear stress to the sample by slowly tilting the bed. As the angle of tilt increases, this generates a shear stress in the powder layer. For deep beds, the location of the shear plane and the angle of tilt α at which failure occurs depend on the width of the bed D[23]. If we restrict our samples to shallow layers of height $h<<D$, it is observed that the width of the bed has no major influence and that powder failure occurs near the base of the sample. We then have

$$\tau_1 \simeq \rho_p \langle \phi \rangle gh \sin \alpha \tag{15}$$

Similarly, the consolidation stress is related to the weight of the sample and to the angle of tilt

$$\sigma_1 \simeq \rho_p \langle \phi \rangle gh \cos \alpha \tag{16}$$

Thus, from the angle at which the sample fails in shear, we calculate the coordinates of one point (σ_1, τ_1) on the yield locus. In order to generate more data for the yield locus we need to be able to vary the compressive stress on the sample. As before, we do this by means of a small remaining gas flow reducing consolidation. If we now tilt the apparatus, the shear stress at the bottom of the sample is given by Eq. 15 since the component of the buoyancy force acting on the shear direction is zero. On the other hand, the consolidation stress σ acting perpendicular to the shear plane is reduced by the gas pressure drop Δp, and so Eq. 16, modified to take account of Δp, becomes

$$\sigma \simeq \rho_p \langle \phi \rangle gh \cos \alpha - \Delta p \tag{17}$$

As the consolidation stress is decreased, the angle of failure decreases and for zero tilt, we recover the measurement of the uniaxial tensile yield stress σ_t. Thus, by combining gas flow and tilt, we can generate a range of conditions of shear stress and normal stress. **Figure 18** shows the incipient yield locus obtained in this way for the Canon CLC500 toner. Two sets of experimental results obtained with experimental toners of different cohesivity are shown in **Figure 19**. For the cases illustrated in **Fig. 19**, the Aerosil concentrations are 0.02% and 0.2% by weight. Clearly, the yield loci of the two materials at low stresses are very different. For a given normal stress, the critical shear stress needed to make the powder flow decreases when the flow additive is increased as a consequence of the decrease of adhesion force.

Another remarkable feature of the yield loci is their convex shape at small stresses. This is a well-known

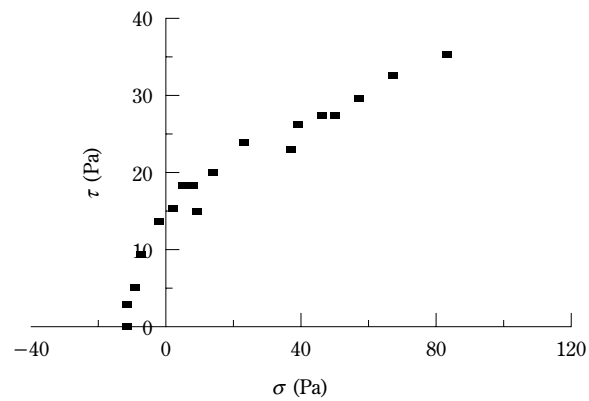

Fig. 18 Yield locus of the Canon CLC700 toner determined by the tilted fluidized bed technique.

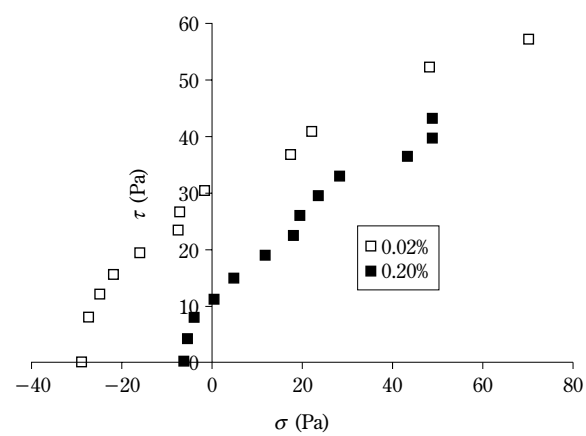

Fig. 19 Yield locus of experimental toners (12.7 μm particle size, 0.02% and 0.2% by weight of Aerosil) determined by the tilted fluidized bed technique.

common aspect of the yield locus of fine powders at low stresses [7]. Moreover, we see that the cohesion c of the powder, defined as the critical shear stress for zero consolidation stress, is comparable to the uniaxial tensile yield stress.

If we approximate the yield loci obtained at high stresses by a Coulomb's linear law (Eq. 1), we see in **Fig. 19** that our results predict an increase of the angle of the internal friction with the percentage of flow conditioner, as observed by Steeneken et al. [37] in potato starch powders, due to the roughening of the powder particles by the additive. We derived the same trend on the effect of additive on the angle of internal friction from experiments where the angle and depth of avalanches were measured in tilted beds of varying width and the results were fitted by a wedge model [23].

In the tilted fluidized bed technique, the yield locus is not defined for a "presheared" sample and the end Mohr circle for steady state flow cannot be determined. Therefore, the initial states in the classical shear testers and our tester are different. Nevertheless, a comparison of the yield loci obtained using our technique with the yield loci obtained from other standard testing devices such as the recently developed ring shear tester [20] is of great interest, and no doubt it will contribute to deepen our understanding of the behavior of powders subjected to very small shear and normal stresses.

4 Conclusions

In this paper we have described a Powder Tester instrument whose main advantages are i) results are operator-insensitive since measurements are automatically taken, and ii) fluidization provides a convenient method to have the sample in a reproducible initial state. Every step in the process is determined by gas flow, and by means of a set of valves and flow controllers, we are able to run the entire process by a computer. The measurements involving gas flow velocity, pressure difference, and bed height are accessed by the same computer, and from these sets of measurements, the values of consolidation stress, average particle volume fraction, and uniaxial tensile yield stress are automatically calculated. An upward/downward-directed gas flow is used for deconsolidating/consolidating the powder, and an ultrasonic device measures the bed height giving an average value of the particle volume fraction. By quasistatically tilting the bed, the SPT also serves to measure the yield shear stresses. This technique is especially feasible to measure the yield locus of cohesive powders, which are difficult to initialize, subjected to very small consolidation stresses.

As a concluding remark we want to stress that the usefulness of the SPT is not just restricted to flowability diagnosis. Our experimental work shows that the tester is a powerful instrument of research in powder technology.

Acknowledgements

This research has been supported by the Xerox Foundation, the Xerox Corporation, and the Spanish Government Agency Ministerio de Ciencia y Tecnologia (DGES) under contract BMF2003-01739. We acknowledge P.K. Watson, M. Morgan, F. Genovesse, A. Ramos, and A. T. Perez for their valuable contributions to this work.

References

[1] B.J. Ennis in *Powders & Grains 97* (Balkema, Rotterdam, 1997) p. 13.

[2] R. Jones, H.M. Pollock, D. Geldart, and A. Verlinden: Powder Technol., **132**, 196 (2003).

[3] A. Castellanos, J.M. Valverde, A.T. Prez, A. Ramos and P.K. Watson: Phys. Rev. Lett, **82**, 1156 (1999).

[4] A. Castellanos, A. Ramos, and J.M. Valverde: *Device and method for measuring cohesion in fine granular media*. Patent no. WO9927345-A. Patent Assignee: University of Seville. Publication date: June 3, 1999. J.M. Valverde, A. Castellanos, A. Ramos, A.T. Perez, M.A. Morgan and P.K. Watson: Rev. Sci. Instrum. **71**, 2791 (2000).

[5] J.M. Valverde, A. Castellanos and M.A.S. Quintanilla: Phys. Rev. Lett. **86**, 3020 (2001). A. Castellanos, J.M. Valverde and M.A.S. Quintanilla: Phys. Rev. E. **64**, 041304 (2001). J.M. Valverde, M.A.S. Quintanilla, A. Castellanos, and P. Mills: Phys. Rev. E **67**, 016303 (2003). J.M. Valverde, A. Castellanos, P. Mills and M.A.S. Quintanilla: Phys. Rev. E **67**, 051305 (2003).

[6] M.A.S. Quintanilla, A. Castellanos, and J.M. Valverde: Phys. Rev. E **64**, 031301 (2001).

[7] J. Schwedes: Granul. Matter **5**, 1 (2003).

[8] Book of ASTM Standards, Part 9, *American Society for Testing and Materials*, Philadelphia, 45, 1978.

[9] D.A. Hall and J.G. Cutress: J. Inst. Fuel, **33**, 63 (1960).

[10] Cole Parmer 1997-1998 catalog, p. 541.

[11] C.M. Iles, Bateson I.D., Walker J.A.: *Rheometer for testing flow characteristics of materials such as powders, liquids and semisolids such as pastes, gels and ointments.* Patent no. EP1102053-A2, May 23, 2001.

[12] R.L. Carr: Chem. Engng, **18**, 163 (1965).

[13] P.K. Watson, J.M. Valverde and A. Castellanos: Powder Technol. **115**, 44 (2001). J.M. Valverde, A. Castellanos and P.K. Watson, Powder Technol., **118**, 240 (2001).

[14] R.L. Carr: Chap. 2, Gas-Solids Handling in Process Industries, Marcel Dekker, NY, 1976.
[15] British Standard 1377, *Methods of tests for soils for civil engineering purposes* (1975).
[16] H.H. Hausner: Int. J. Powder Metallurgy, **3**(4), 7 (1967).
[17] C.A. Coulomb: *Mémoires de Mathéematics et de Physique présentés a l'Acadéemie des Sciences par divers savants et lus dans les assemblées, Année 1773* (Académie Royale des Sciences, Paris, 1776) Vol. 7, p. 343.
[18] J. Schwedes: *Fließverhalten von Schüttgütern in Bunkern*., Verlag Chemie GmbH, Weinheim, 1968.
[19] Institute for Reference Materials and Measurements. Directorate General Joint Research Centre of the European Commission.
[20] D. Schulze and A. Wittmaier: Chem. Eng. Technol. **26**, 2 (2003).
[21] L. Svarovsky: *Powder Testing Guide: Methods of Measuring the Physical Properties of Bulk Powders* (Elsevier Applied Science, England 1987).
[22] *Classification and Symbolization of Bulk Materials* ISO 3435-1977-E-.
[23] J.M. Valverde, A. Castellanos, A. Ramos and P.K. Watson: Phys. Rev. E **62**, 6851 (2000).
[24] M.A.S. Quintanilla, J.M. Valverde, A. Castellanos, R.E. Viturro: Phys. Rev. Lett. **87**, 194301 (2001).
[25] Kaye, B.H., Gratton-Liimatainen, J. and Faddis, N.: Part. Part. Syst. Charact., **12**, 232 (1995).
[26] Poole T.A.: *Apparatus for determining powder flowability*. Patent no. WO9738297-A1, Oct 16, 1997.
[27] J.M. Valverde, A. Ramos, A. Castellanos and P.K. Watson: Powder Technol., **97**, 237 (1998).
[28] Y. Shimada, Y. Yonezawa, H. Sunada, R. Nonaka, K. Katou, and H. Morishita: KONA **20**, 223 (2002).
[29] T. Hiroyuki: *Method and instrument for measuring adhesion of granular body*. Patent no. JP3269340, Nov 29, 1991.
[30] H. Schubert: Powder Technol. **37**, 105 (1984).
[31] J.M. Valverde, A. Castellanos and M.A.S. Quintanilla: Contemp. Phys. **44**, 389 (2003).
[32] P.C. Carman: Trans. Inst. Chem. Engrs. **15**, 150 (1937).
[33] S.C. Tsinontides and R. Jackson: J. Fluid Mech., **255**, 237 (1993).
[34] J.F. Richardson and W.N. Zaki: Trans. Inst. Chem. Engrs. **32**, 35 (1954).
[35] K. Rietema: *The Dynamics of Fine Powders* (Elsevier, London 1991).
[36] A. Castellanos, J.M. Valverde, and P.K. Watson: ZAMM **80**, S423 (2000).
[37] P.A. Steeneken and A.J. Woortman: Powder Technol. **47**, 239 (1986).

Author's short biography

Antonio Castellanos Mata

Antonio Castellanos received his doctoral degree in nuclear physics in 1972. Actually he is Professor of Electromagnetism at the University of Seville, Spain. His current research interests are in the coupling of electric fields to fluids (electrohydrodynamics, EHD), in control of bio-particles and liquids in microelectrodes structures (AC electrokinetics and EHD in MEMS), in gas discharges (ozonizers, pollution control), and in the physics of cohesive granular media.

José Manuel Valverde Millán

José Manuel Valverde Millán obtained a Batchelor Sience degree in Physics at the University of Seville in Spain in 1993, and a Ph.D. in Physics from the same University in 1997. He teaches electromagnetism at the department of Electronics and Electromagnetism, University of Seville. His main research topic is the fundamental physics of cohesive powders. He has published around 25 papers in international journals and is co-author of the patent on the Seville Powder Tester described in this paper. In most of his research projects he has worked in collaboration with Xerox Co.
He is married with Isabel, has a beautiful little daughter (Sofia) and a beloved 13 years old son (Manuel), and lives in San José de La Rinconada (Spain).

Miguel Angel Sánchez Quintanilla

Miguel Angel Sánchez Quintanilla received the B.S. degree in Physics from the University of Seville in 1998 and the Ph.D. degree in 2003 also in the University of Seville. His research interests are in the mechanics of cohesive granular materials and fluidization of powders, and in particular the relation between the mesoscopic and continuum approaches.